Optimal Mass, Spin, and Orientation Parameters for Detecting Higher Order Gravitational-wave Modes from Binary Black Hole Mergers

Mahlet Shiferaw*
Harvard-Smithsonian Center for Astrophysics, Cambridge, MA 02138

Alan Weinstein† and Liting Xiao‡
LIGO, California Institute of Technology, Pasadena, CA 91125

(LIGO Collaboration)

(Dated: July 11, 2019)

Thus far, the Advanced Laser Interferometer Gravitational-Wave Observatory (aLIGO) and Advanced Virgo have detected gravitational waves (GWs), or ripples in the curvature of spacetime, from dozens of binary black hole (BBH) and binary neutron star (BNS) mergers. In order to detect the GWs from these mergers, aLIGO data are optimally searched using matched filtering against a bank of model waveform templates which are well-described by General Relativity (GR). Currently, such searches only utilize waveforms for the dominant Y_{22} mode, neglecting higher order modes (HOMs). However, these HOMs carry information about the source and the radiation it emits, and are therefore of great interest to study. Our goal is to identify the presence of HOMs in signals found in the data in order to test GR. Using a newly-released catalog of BBH simulations with HOMs developed by the Simulating eXtreme Spacetimes (SXS) Collaboration, we will assess the capabilities of aLIGO for detecting HOMs. Such detections are currently very unlikely, as HOMs are at least half an order of magnitude lower in amplitude than the dominant mode, and tend to lie outside of LIGO's sensitive frequency band for low-mass systems. Constrained by this strain sensitivity, we aim to determine the range of BBH mass, spin, and orbital orientations which optimizes the likelihood of detecting HOMs. We will do so by injecting SXS waveforms with HOMs into aLIGO recolored noise and analyzing the results, thus paving the way for a powerful test of GR in the strong-field highly dynamical regime.

Usage: Caltech SURF Interim Report I.

I. INTRODUCTION

Gravitational waves (GWs) are violent ripples of spacetime created by catastrophic events such as colliding black holes, supernovae, and merging neutron stars. Predicted by physicist Albert Einstein in his Theory of General Relativity (GR) in 1916, Einstein's field equations show that such massive accelerating objects cause distorted waves to travel through the fabric of spacetime at the speed of light [1, 2].

Despite this breakthrough, GWs were not detected for another century, until September 14th, 2015, when the two detectors of the Advanced Laser Interferometer Gravitational-Wave Observatory (aLIGO) both observed the first GW signal, GW150914, at exactly 09:50:45.4 UTC [3]. Caused by a binary black hole (BBH) merger, GW150914 was detected during the first observing run (O1) of Advanced LIGO, which ran from September 12th, 2015 to January 19th, 2016 [4]. The second observing run (O2) ran from November 30th, 2016 to August 25th, 2017, and on August 1st, 2017, the Advanced Virgo detector joined O2, allowing for three detectors to simultaneously search for GWs for the first time in history [5].

This makes aLIGO the world's largest, most complex, and most sensitive interferometer, designed purely for the detection of these miniscule oscillations in spacetime. Soon, a global network of detectors will join aLIGO, with three detectors having already been built in Japan, Italy, and Germany [6], and a third LIGO detector to be built in India. Furthermore, the third observing run (O3) of Advanced LIGO and Virgo began in April 2019, and is planned to continue throughout the summer of 2019 for one calender year [7]. As such, gravitational waves are ushering in a new era of multi-messenger astronomy, in which astrophysicists have an entirely new way of viewing and understanding the cosmos.

A. Detection of Gravitational Waves

These developments represent an exciting opportunity to take advantage of the increased number of detections and enhanced signal-to-noise ratio (SNR), both of which will presumably only increase as the years go by. The implications of these improvements are numerous, as GWs carry not just energy and momentum, but crucial information about the structure of their sources. In partic-

* mshiferaw@college.harvard.edu
† ajw@caltech.edu
‡ lxxiao@caltech.edu

ular, a quasi-circular coalescing compact binary is completely characterized by fifteen parameters, which include the mass of each object in the merger, their spins, and their orbital orientation [8].

During an observing run, aLIGO continually takes in data, which means that these data must simultaneously be scrutinized for possible GW events. Events are thus detected using a technique called matched filtering, which selects the optimal model waveform for an observed signal from a *template bank*. Because the key parameters which describe a waveform, such as the amplitude, masses, spins, fiducial reference time, and orbital phase, are not known before matched filtering begins, such template banks search through parameter space to construct thousands of possible gravitational waveforms [9].

Matched filtering thus searches the data for resemblance to each template, for each time step dt of data. If a time step has an SNR $\gtrapprox 8$, further investigations are done using Bayesian inference, a process which takes the model waveform and, given a range of parameters and expectations for noise, produces posterior distributions on the input parameters. With this, refined parameters can be extracted from any signal with a high enough SNR.

B. Higher Order Modes

During matched filtering, current model waveforms are restricted so that they only include the leading order Y_{22} mode of the waveform. This is because the full waveform, which includes the sum of all modes, depends on the viewing angle of the observer, something that is not known at the time of the search. This restriction, while providing reasonable estimations at a far less computationally expensive rate, comes at a cost: as both Payne et al. and Kumar et al. have shown, including HOMs provides tighter constraints on the source parameters than the fundamental $l = 2$ mode [10, 11].

This has three main benefits: including HOMs in our calculations will allow this parameter estimation procedure to become much more precise, thus greatly furthering our understanding of these GW sources. Furthermore, using waveforms with HOMs will likely increase the similarities between template and data during matched filtering, thus boosting aLIGO's detection confidence. Finally, including HOMs makes it possible to test for their presence in the signal found in the data, a powerful test of GR as the theory of strong gravity and GWs.

Unfortunately, there is yet another difficulty in including these HOMs in the parameter estimation process: they are at least half an order of magnitude fainter than the dominant Y_{22} mode, and tend to lie outside of aLIGO's sensitivity frequency band for low-mass systems. This has a two-fold effect, in both parameter estimation and matched filtering. This means that no HOMs have been detected as of yet, and will likely not be detected until aLIGO's sensitivies improve, or until a detector happens to observe a close-by event with high SNR.

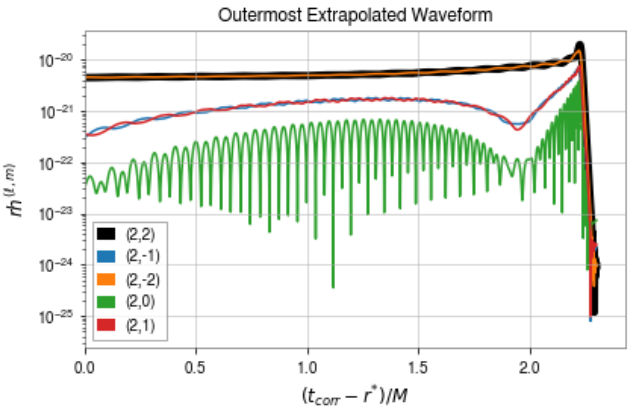

FIG. 1. The real strain amplitude of the fundamental Y_{22} mode, along with four of the strongest HOMs. Despite this selection, the HOMs are at least half an order of magnitude weaker in amplitude than the dominant mode, and progressively become more and more noisy. The x-axis is truncated here to remove untrustworthy simulation data.

As a result, in this project we aim to determine exactly how high in SNR an event detection needs to be in order to present statistically significant evidence for HOMs. In assessing the full extent of aLIGO's capabilities for detecting these HOMs, we will be able to better inform future detections, especially as aLIGO continues to be upgraded.

We will accomplish this by injecting simulated gravitational waveforms, both with and without HOMs, into aLIGO recolored noise and analyzing the results. We will use waveforms from the Simulating eXtreme Spactimes (SXS) newly-released template bank for BBH mergers, which includes the dominant mode as well as HOMs [12]. This will then allow us to determine the optimal parameter range of source merger mass, spin, and orbital orientation for detecting HOMs, as constrained by aLIGO's sensitivies. Because HOMs are predicted by GR but have not yet been detected, this will also allow us to perform unique and powerful tests on GR in the strong-field, highly dynamical regime.

II. METHODS

This project will require the use of SXS's newly-released template bank of waveforms with HOMs included, as well as `Bilby`, a user-friendly Bayesian inference library [13], and the `GWpy` software package in Python [14]. Our approach consists of an idealized initial analysis, described in Section II A, and a more realistic analysis, described in Section II B.

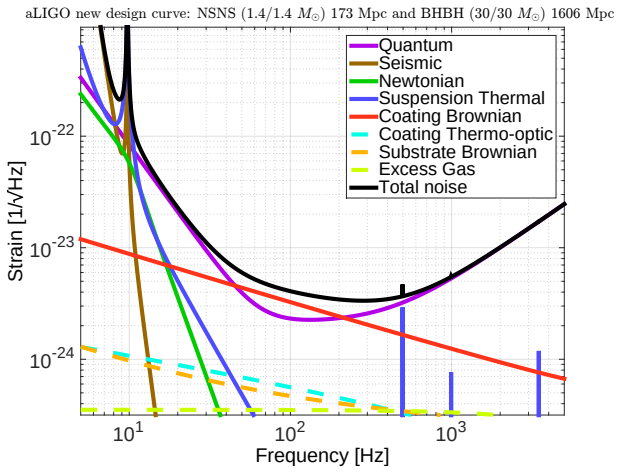

FIG. 2. The updated aLIGO sensitivity design curve, which takes into account coating thermal noise. In black is the total noise of the design curve. Figure courtesy of LIGO Scientific Collaboration.

A. Idealized Approach

In this project, we will begin by first establishing that there is indeed a visible and quantitative difference between waveforms with HOMs and without HOMs. In Figure 1, the waveform for `SXS:BBH:0444`, a BBH merger with mass ratio 1.250 and orbital inclination 1.484×10^{-2}, is depicted. The real amplitude of the strain is plotted for the dominant Y_{22} mode, as well as four of the strongest HOMs. The amplitude for the $Y_{2\pm1}$ mode is already half an order of magnitude smaller than the dominant mode, and subsequent HOMs tend to have increasingly weaker signals.

The next step in the process is to Fourier Transform these waveforms, and plot each of these modes as a function of frequency, rather than time. Finally, plotting the sum of all of these modes will result in the full waveform. Our goal is to plot this full waveform, in addition to the dominant waveform, against aLIGO's design sensitivity curve in order to show the full range of frequencies in which the detectors can actually observe HOMs. This design curve, known as Amplitude Spectral Density (ASD), is depicted in Figure 2.

Plotting these three curves together should reveal the delicate balance which exists between total merger mass, orbital orientation, and spin. A lower total mass increases the frequency of the merger and shifts the strain amplitude to the right, while the strain amplitude increases as the merger becomes more face-on. Adding spin will complicate this even further, as a merger might also precess about its orbital plane, and thus the observer's viewing angle with respect to the line of sight [15]. The effect of this precession on the observed waveform is better seen edge-on rather than face-on, but strain amplitudes are highest for face-on systems.

Afterwards, we will plot the waveform peak frequency as a function of time and compute the optimal SNR as a function of mass ratio and orientation angle. More quantitatively, we will compute the overlap integral between the dominant Y_{22} mode and waveform with HOMs in order to find where the overlap is smallest. Because an overlap integral is essentially an inner product, if h_1 and h_2 are identical, then O will go as 1. The less they have in common, the smaller O is, indicating that there is a high likelihood of detection, and the HOMs will be able to be distinguished from the dominant mode. The overlap integral is shown in Equation 1 below, where $h_1(f)$ and $h_2(f)$ are the waveform with and without HOMs, and PSD is the Power Spectral Density, referring to the square of the total design noise curve depicted in Figure 2:

$$\mathrm{PSD} = \mathrm{ASD}^2 \tag{1a}$$

$$\langle h_1|h_2\rangle = \int df \frac{h_1(f)\,h_2^*(f)}{\mathrm{PSD}(f)} \tag{1b}$$

$$O = \frac{\langle h_1|h_2\rangle}{\sqrt{\langle h_1|h_1\rangle\langle h_2|h_2\rangle}} \tag{1c}$$

B. Realistic Approach

This overlap integral will inform us as to which HOMs are statistically significant and which are negligible. Experimenting with different masses and spins will also visually guide us to which combination is optimal, allowing us to gain an intuition for the SNR. However, it is important to note that the total noise curve depicted in Figure 2 is an idealization of the noise curve. Noise, by definition, is random in time, but because the PSD is an average of many noise realizations, it is constant in the frequency domain. In order to find the optimal range of parameters in a more realistic fashion, we will need to work in the time domain of the noise.

Therefore, rather than working with the idealized LIGO design curve described in Section II A, we will inject simulated signals with a broad range of parameters into aLIGO recolored noise. Finally, we will use `Bilby` to obtain the Bayesian odds ratio, or Bayes factor, for waveforms with and without HOMs. This ratio will quantify the degree to which we can say that HOMs are present in the simulated data, allowing us to proceed with model selection, fit the waveform, and extract the desired fifteen parameters from detected GWs. These are composed of the following intrinsic parameters:

(1) the source frame component masses m_1 and m_2

(2) the source frame component spin vectors $\vec{\chi}_1$ and $\vec{\chi}_2$,

as well as the following extrinsic parameters:

(3) the luminosity distance d_L

(4) the source's sky localization $\Delta\Omega$, characterized by its right ascension (RA) and right declination (Dec)

(5) the polar angle ι and polarization angle ψ of the orientation of the binary orbit with respect to the line-of-sight of the observer

(6) the coalescence time t_c at which the signal from the merger reaches the center of the Earth

(7) the phase of the signal ϕ_c at the moment of coalescence

The observer's viewing angle to the source ι is a key parameter which differentiates the full waveform from the restricted waveform. For the latter, ι is indeed an extrinsic parameter, meaning that only the overall amplitude is dependent on it. In contrast, for the full waveform with HOMs, ι becomes an intrinsic parameter upon which the shape of the waveform is also dependent.

C. Relevant Equations

The characteristic dimensionless gravitational wave strain amplitude h for a source of mass M located at a distance r away can be described by Equation 2. In this notation, Q refers to the quadrupole moment of the source event, ω is its angular frequency of oscillation, μ is the reduced mass, a is the separation between the two source frame component masses m_1 and m_2, and M is the total mass of the merger [16]:

$$h \sim \frac{G}{c^4}\frac{1}{r}\frac{d^2Q}{dt^2}, \quad Q = -\omega^2\mu a^2, \quad \mu = \frac{m_1 m_2}{M} = \frac{m_1 m_2}{m_1 + m_2} \tag{2}$$

The angular frequency ω can be rewritten in terms of the orbital period, using Kepler's third law in Equation 3:

$$\omega = 2\pi f_{\text{orb}} = \frac{2\pi}{\tau_{\text{orb}}}, \quad {\tau_{\text{orb}}}^2 = \frac{4\pi^2}{G(m_1+m_2)}a^3 = \frac{4\pi^2}{GM}a^3 \tag{3}$$

Here, $f_{\text{GW}} = 2f_{\text{orb}}$, where f_{GW} refers to the frequency of the gravitational wave and f_{orb} is the orbital frequency. Equation 2 can thus be rewritten as Equation 4, where R_{Schw} is the Schwarzschild radius of the source and η is a unitless mass factor:

$$h \sim -\frac{GM}{c^2 r}\frac{G\mu}{c^2 a} \sim -\frac{\eta {R_{\text{Schw}}}^2}{4ra} \tag{4a}$$

$$\eta = \frac{\mu}{M} = \frac{m_1 m_2}{M^2}, \quad R_{\text{Schw}} = \frac{2GM}{c^2} \tag{4b}$$

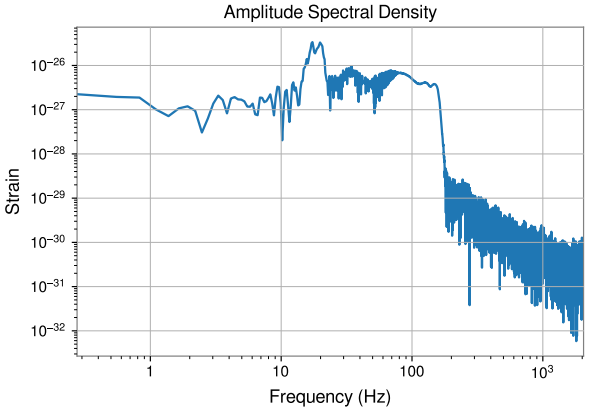

FIG. 3. The waveform for the dominant mode of `SXS:BBH:0444`, Fourier-Transformed into frequency space.

The strain amplitude in Equation 4a can also be written in terms of the chirp mass $\mathcal{M}$, as defined by Equation 5 below:

$$h \sim -\frac{(G\pi f_{\text{GW}})^{4/3}}{c^4 r}\mathcal{M}^{5/6}\eta^{1/2}, \quad \mathcal{M} = M\,\eta^{3/5} \tag{5}$$

From these equations, it is clear that GWs can inform us about many features of the source event. Source parameters from newly detected GWs can thus be extracted using Bayesian parameter estimation, a method of mathematical modeling which is used to model real phenomena. In contrast to the classical frequentist approach, which chooses a value for some input parameter θ that maximizes the likelihood of the observed data, Bayesian parameter estimation holds the observed evidence as fixed and instead infers a Posterior Density Function (PDF) for θ [17]. Bayesian inference is a crucial tool in all of modern science, but is particularly useful in gravitational wave astronomy: a black hole can be completely characterized by its mass and spin vector, and the gravitational waveform from a BBH by a total of fifteen parameters, described in Section II B [18].

There are a number of parameters which can be derived from these input parameters, including the final source frame mass M_f, the final spin a_f, the radiated energy E_{rad}, the peak luminosity l_{peak}, the redshift z, the chirp mass $\mathcal{M}$, and the dimensionless effective aligned spin χ_{eff}. The latter is described by Equation 6, where $\hat{L}_N$ is the Newtonian angular momentum of the source event:

$$\chi_{\text{eff}} = \frac{(m_1\vec{\chi}_1 + m_2\vec{\chi}_2)\cdot\hat{L}_N}{M} \tag{6}$$

III. PROGRESS

So far, I am still on the "idealized" portion of my project. I have produced the plot seen in Figure 1, which

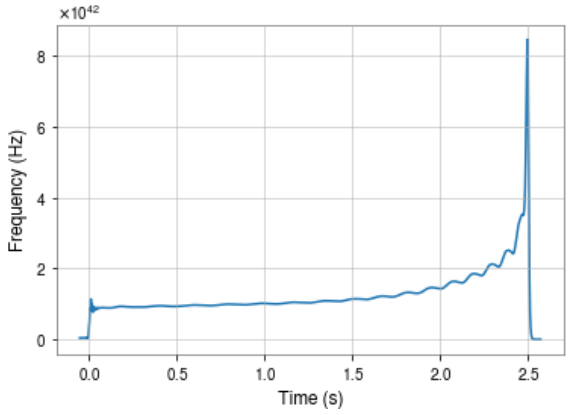

FIG. 4. My initial attempt at plotting frequency as a function of time. Currently, the units are for the amplitude are far too high and are not correct.

depicts the various modes of a simulated BBH merger from the SXS catalog. I am currently working on computing the Fourier Transform of the dominant Y_{22} waveform, as depicted in 3, in order to plot it on top of the LIGO noise design curve, shown in Figure 2. However, because the former is unitless, I must first convert the y-axis to $1/\sqrt{Hz}$.

I have also begun to make a plot of frequency against time for this waveform; my initial attempt is depicted in Figure 4. My immediate next steps moving forward will be to repeat this process for each of the HOMs, and finally sum up the modes to obtain the full waveform. I aim to complete this by the end of the week. Next week, I will begin working on calculating the overlap integral described by Equation 1.

IV. CHALLENGES

The biggest challenge thus far has been in starting my new project from scratch two weeks into the program. As a result, I anticipate that it will be difficult to complete all of our goals in time before the program ends.

Other challenges I have encountered mainly revolve around getting acquainted with technical methods, such as downloading the appropriate software, learning how to perform a Fourier Transform on a simulated waveform from the SXS catalogue, and figuring out how to convert the units in the ASD from strain to strain/$\sqrt{(Hz)}$. Lastly, I have faced issues with deriving conceptual terms, such as expression for frequency in terms of time, the Innermost Stable Circular Orbit (ISCO) radius, and frequency at ISCO. Fortunately, all of these challenges can simply be solved by spending more time on the project.

Moving forward, I anticipate that the most challenging parts of my project will include learning how to sum the modes in a waveform, as I will need to include parameters such as the viewing angle, as well as finding the optimal SNR by calculating the overlap integral. Moreover, I expect great difficulty in trying to understand quaternions.

ACKNOWLEDGEMENTS

I would like to thank Alan Weinstein for serving as my research advisor on this project, as well as Jonah Kanner and Liting Xiao for their guidance. I would also like to thank the Caltech Student Faculty Program (SFP) for organizing the LIGO SURF program. Finally, I would like to thank the National Science Foundation (NSF) for their funding.

[1] Einstein A. Approximative Integration of the Field Equations of Gravitation. Sitzungsber Preuss Akad Wiss Berlin (Math Phys). 1916;1916:688–696.

[2] Einstein A. ber Gravitationswellen. Sitzungsber Preuss Akad Wiss Berlin (Math Phys). 1918;1918:154–167.

[3] Abbott BP, Abbott R, Abbott TD, Abernathy MR, Acernese F, Ackley K, et al. Observation of Gravitational Waves from a Binary Black Hole Merger. Phys Rev Lett. 2016 Feb;116:061102. Available from: https://link.aps.org/doi/10.1103/PhysRevLett.116.061102.

[4] The LIGO Scientific Collaboration, the Virgo Collaboration, Abbott BP, Abbott R, Abbott TD, Abraham S, et al. GWTC-1: A Gravitational-Wave Transient Catalog of Compact Binary Mergers Observed by LIGO and Virgo during the First and Second Observing Runs. arXiv e-prints. 2018 Nov;p. arXiv:1811.12907.

[5] Acernese F, Agathos M, Agatsuma K, Aisa D, Allemandou N, Allocca A, et al. Advanced Virgo: a second-generation interferometric gravitational wave detector. Classical and Quantum Gravity. 2015 Jan;32(2):024001.

[6] Abbott BP, Abbott R, Adhikari R, Ajith P, Allen B, Allen G, et al. LIGO: the Laser Interferometer Gravitational-Wave Observatory. Reports on Progress in Physics. 2009 Jul;72(7):076901.

[7] Turpin D, Wu C, Han XH, Xin LP, Antier S, Leroy N, et al. The mini-GWAC optical follow-up of the gravitational wave alerts: results from the O2 campaign and prospects for the upcoming O3 run. arXiv e-prints. 2019 Feb;p. arXiv:1902.08476.

[8] Cai RG, Cao Z, Guo ZK, Wang SJ, Yang T. The Gravitational-Wave Physics. arXiv e-prints. 2017 Mar;p. arXiv:1703.00187.

[9] Babak S, Balasubramanian R, Churches D, Cokelaer T, Sathyaprakash BS. A template bank to search for gravitational waves from inspiralling compact binaries: I. Physical models. Classical and Quantum Gravity. 2006 Sep;23(18):5477–5504.

[10] Payne E, Talbot C, Thrane E. Higher order gravitational-wave modes with likelihood reweighting. arXiv e-prints. 2019 May;p. arXiv:1905.05477.

[11] Kumar P, Blackman J, Field SE, Scheel M, Galley CR, Boyle M, et al. Constraining the parameters of GW150914 and GW170104 with numerical relativity surrogates. Phys. Rev. D. 2019 Jun;99(12):124005.

[12] Boyle M, Hemberger D, Iozzo DAB, Lovelace G, Ossokine S, Pfeiffer HP, et al. The SXS Collaboration catalog of binary black hole simulations. arXiv e-prints. 2019 Apr;p. arXiv:1904.04831.

[13] Ashton G, Hübner M, Lasky PD, Talbot C, Ackley K, Biscoveanu S, et al. BILBY: A User-friendly Bayesian Inference Library for Gravitational-wave Astronomy. . 2019 Apr;241(2):27.

[14] Macleod D, Urban AL, Coughlin S, Massinger T, paulaltin, Areeda J, et al.. gwpy/gwpy: 0.14.2; 2019. Available from: https://doi.org/10.5281/zenodo.2603187.

[15] Dietrich T, Bernuzzi S, Brügmann B, Ujevic M, Tichy W. Numerical relativity simulations of precessing binary neutron star mergers. Phys. Rev. D. 2018 Mar;97(6):064002.

[16] Centrella JM. What can we learn about cosmic structure from gravitational waves? In: Holt SH, Reynolds CS, editors. The Emergence of Cosmic Structure. vol. 666 of American Institute of Physics Conference Series; 2003. p. 337–346.

[17] Eshky A. Bayesian Methods of Parameter Estimation Aciel Eshky; 2009. .

[18] Thrane E, Talbot C. An introduction to Bayesian inference in gravitational-wave astronomy: Parameter estimation, model selection, and hierarchical models. . 2019 Mar;36:e010.